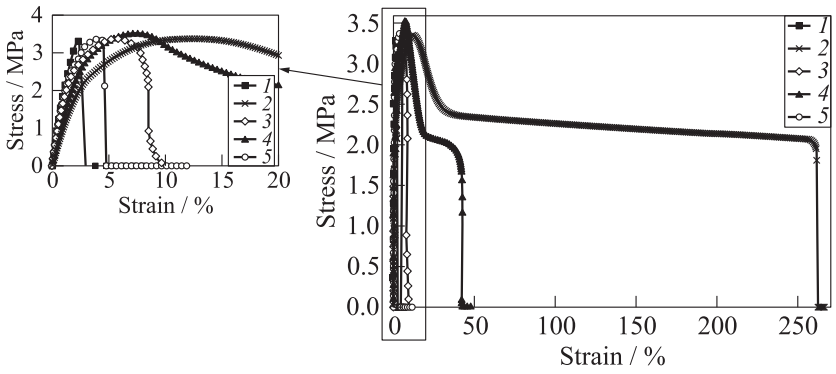

Figure 13 Effects of polymer mass fraction on the elongation at break (T = 8 °C and 50 mm/min): *1* — S05G; *2* — S10G; *3* — S15G; *4* — S20G; and *5* — S30G

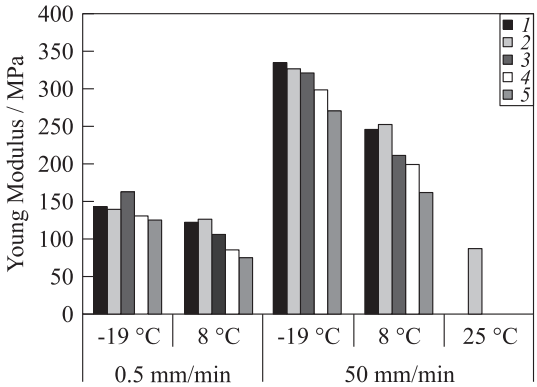

Figure 14 Young Modulus trend of SEBS-based formulations with temperature and elongation speed: *1* — S05G; *2* — S10G; *3* — S15G; *4* — S20G; and *5* — S30G

Table 4 Young Modulus with standard deviation (in MPa) obtained with tensile tests at −19 and 8 °C and 0.5 and 50 mm/min for SEBS-containing formulations

Rate, mm/min	T_{storage}, °C	GW	S05G	S10G	S15G	S20G	S30G
0.5	8	119.2 ± 17.32	123.1 ± 8.0	127.1 ± 1.1	106.7 ± 12.2	86.8 ± 2.1	75.3 ± 5.7
	−19	—	143.1 ± 17.7	141.7 ± 16.1	163.4 ± 12.3	130.6 ± 5.2	126.2 ± 6.5
50	8	—	246.1 ± 23.6	252.8 ± 19.2	211.7 ± 14.6	200.1 ± 4.2	162.6 ± 11.0
	−19	—	334.5 ± 13.9	327.4 ± 36.1	320.7 ± 14.2	299.4 ± 16.6	269.8 ± 2.3

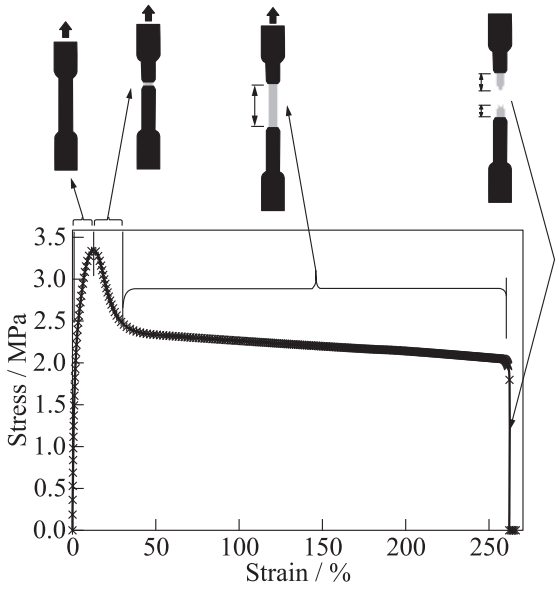

Figure 15 The S30G stress/strain trace divided into four main sections linked with a schematic representation of the dog-bone sample shape evolution

In Fig. 13, S15G shows a stress/strain trace typical of brittle materials: immediately after the achievement of the maximum stress, the break of the dog-bone sample is observed. This is probably due to the polymer low concentration which is not able to change the typical brittle behavior of the paraffin wax. S30G has a quite different behavior showing a ductile stress/strain trace. When the stress reaches the maximum value (3.3 MPa), a change in the mechanical behavior of the material is observed as the sample is not more able to tolerate the stress. When the strain increases, the stress decreases until the break point (at 262 percent strain).

Figure 15 shows how the shape of the dog-bone sample changes with the strain. Four main parts can be observed considering the stress/strain trace and each one is linked to a particular shape of the sample. The first part (0%–12%) shows a linear stress/strain trace, the sample shape is regular, the color is dark. The fast decrease of the stress in the second part (12%–32%) is linked to the appearance of a small striction, the color becomes grey. In the third part, both the length of the striction and the strain grow (32%–260%), until they reach the maximum at the break point. The color of the restriction of the dog bone is grey because of the presence of wax crystals on the sample external surface. This behavior is due to the straightening (deentanglement) of the polymer molecules because of the increase of strain, which involves the

expulsion of wax crystals towards the surface. Considering the low temperature of the sample (8 °C), all the styrenic micelles are cohesive; only the elastomeric midblocks operate.

6 PROPERTIES OF TRADITIONAL HTPB- AND PARAFFIN-BASED FUELS

A comparison of fuel properties measured in this work with mechanical properties of HTPB and thermal and mechanical properties of different paraffin-based fuel formulations is reported in Tables 5 and 6, respectively. The comparison is affected by the composition of the fuel, by different standards and reference values, which strongly can change the measured values. For this reason, the comparison aims to compare the orders of magnitude and to show where improvements are needed for a successful use of paraffin-based fuels in space

Table 5 Mechanical properties of HTPB-based fuels (T_{test} — test temperature; σ_m — maximum stress; ε_m — elongation at maximum stress; E — Young Modulus; and ND — not determined)

Material	T_{test}, °C	σ_m, MPa	ε_m, %	E, MPa	Method	Reference
HTPB R45M	−30	2.0	25.0	24.3	ND	[30]
HTPB R45M	20	0.9	26.0	5.4	ND	[30]
HTPB R45M*	23	0.6–0.9	190–430	0.2–0.5	ND	[31]
HTPB**	23	2.1–21.6	260–480	—	ASTM D412	[32]

*NCO content varying between 4.9% and 9%.

**NCO/OH ranging from 1.0 and 1.2.

Table 6 Mechanical properties of paraffin-based fuels

Material	T_{test}, °C	T_{mp}, °C	σ_m, MPa	ε_m, %	E, MPa	Method	Reference
Wax	—	56–58	1.2	2.3	24.3	ND	[33]
Wax	25	53	0.8	12.0	61.4	ASTM D639-95	[34]
Wax	15	48	170.0	5.3	171.0	ASTM D639-95	[35]
	25	48	80.0	13.1	81.6	ASTM D639-95	[35]
	30	48	42.1	105.3	60.5	ASTM D639-95	[35]
Wax*	—	54–64	0.9–1.0	0.4–0.6	190–260	ASTM D412	[36]
Wax**	—	99–104	4.0–12.5	90–800	100–1000	ASTM D412	[36]
	—	53–55	0.55	up to 260	75–335	UNI-EN-ISO 527	Present work

*Several paraffin wax formulations.

**Low-density polyethylene.

propulsion applications. The measured properties for the formulations studied in this work show that the investigated fuels can compete with traditional HTPB-based fuels and are in good agreement with paraffin-based formulations discussed in the literature. Further research activities could improve the values for σ_m (maximum stress), considering that increase of σ_m leads to a decrease of ε_m (elongation at maximum stress). A balance between these two properties is linked to the specific mission requirements. According to the Young Modulus, the measured values, which are in the range 75–335 MPa, comply with the needs.

On the whole, the investigated formulations show good properties for their use as solid fuels in hybrid propulsion applications.

7 CONCLUDING REMARKS

The paper discusses the characterization results of paraffin-based fuels mixed with a styrene-based thermoplastic elastomer used as strengthening material. The DSC and TGA-DTA techniques, a parallel plate rheometer, a Couette viscosimeter, gas-cromatography, and uniaxial tensile tests were used to characterize pure paraffins and their blends.

The overlapping of DSC thermographs and elastic modulus traces confirms the presence of critical temperature values which explain the rheological behavior of paraffin wax blended with different mass fractions of SEBS-MA.

For GW-based blends such as S15G and S30G, two critical temperatures can be seen dividing G' trace into three main areas. The DSC tests point out that the peak where GW melting occurs is at 54 °C. If the mass fraction of the polymer is larger than 15%, the mixture is liquid at higher temperatures, negatively affecting the regression rate behavior.

The materials with a polymer content lower than 15% (S05G and S10G samples) show a behavior typical for rigid and brittle materials. As the SEBS mass fraction increases, the elongation at break increases with a not linear trend. A higher content of thermoplastic polymer involves a decrease of the Young Modulus. A more significant decrease of the Young Modulus (51%–63%) is observed when the fuel temperature is higher (here, 8 °C) and a lower decrease (13%–24%) when the temperature is low (−19 °C). The Young Modulus values are higher for each formulation when the sample temperature decreases (from 8 to −19 °C).

Considering ageing effects, for the three-week aged S15G sample, the limit temperature (T_l) was almost 6 °C higher than that of the fresh mixture.

On the whole, the formulations investigated in this work show suitable properties for their use as low melting temperature solid fuels in hybrid rockets applications.

REFERENCES

1. Chiaverini, M. J., N. Serin, D. Johnson, Y. C. Lu, K. K. Kuo, and G. A. Risha. 2000. Regression rate behavior of hybrid rocket solid fuels. *J. Propul. Power* 16(1):125–132.
2. Karabeyoglu, M. A., B. J. Cantwell, and D. Altman. 2001. Development and testing of paraffin-based hybrid rocket fuels. AIAA Paper No. 2001-4503.
3. Karabeyoglu, M. A., G. Zilliac, B. J. Cantwell, S. DeZilwa, and P. Castellucci. 2004. Scale-up tests of high regression rate paraffin-based hybrid rocket fuels. *J. Propul. Power* 20(6):1037–1045.
4. Karabeyoglu, M. A., and B. J. Cantwell. 2002. Combustion of liquefying hybrid propellants: Part 2. Stability of liquid films. *J. Propul. Power* 18(3):621–630.
5. Maruyama, S., T. Ishiguro, K. Shinohara, and I. Nakagawa. 2011. Study on mechanical characteristics of paraffin-based fuel. *47th AIAA/ASME/SAE/ASEE Joint Propulsion Conference & Exhibit*. San Diego, CA.
6. Prasman, E. 1997. Morphology and mechanical behavior of oriented blends of styrene–isoprene–styrene triblock copolymer and mineral oil. Massachussetts Institute of Technology. Master Thesis.
7. Kim, J. K., M. A. Paglicawan, and M. Balasubramanian. 2006. Viscoelastic and gelation studies of SEBS thermoplastic elastomer in different hydrocarbon oils. *Macromol. Res.* 14(3):365–372.
8. Zhang, Q., S. Song, J. Feng, and P. Wu. 2012. A new strategy to prepare polymer composites with versatile shape memory properties. *J. Mater. Chem.* 22:24776.
9. Royon, L., and G. Guiffant. 2001. Heat transfer in paraffin oil/water emulsion involving supercooling phenomenon. *Energ. Convers. Manage.* 42:2155–2161.
10. Chazhengina, S. Y., E. N. Kotelnikova, I. V. Filippova, and S. K. Filatov. 2003. Phase transition of n-alkanes as rotator crystals. *J. Mol. Struct.* 647:243.
11. Alcazar-Vara, L. A., and E. Buenrostro-Gonzalez. 2013. Liquid–solid phase equilibria of paraffinic systems by DSC measurements. *Applications of calorimetry in a wide context — differential scanning calorimetry, isothermal titration calorimetry and microcalorimetry*. Ed. A. A. Elkordy. InTech. Ch. 11. 253–276. doi: 10.5772/54575.
12. Seno, J., and T. P. Selvin. 2006. Thermal and crystallisation behaviours of blends of polyamide 12 with styrene–ethylene/butylene styrene rubbers. *Polymer* 47:6328–6336.
13. Zheng, M., and W. Du. 2006. Phase behavior, conformations, thermodynamic properties, and molecular motion of multicomponent paraffin waxes: A raman spectroscopy study. *Vib. Spectrosc.* 40:219–224.
14. Reynders, K., N. Mishenko, and K. Mortensen. 1995. Stretching-induced correlations in triblock copolymer gels as observed by small-angle scattering. *Macromolecules* 28:8699.
15. Laurer, J. H., R. Bukovnik, and R. J. Spontak. 1996. Morphological characteristics of SEBS thermoplastic elastomer gels. *Macromolecules* 29:5760.

16. Kleppinger, R., M. van Es, N. Mishenko, M. H. J. Koch, and H. Reynaers. 1998. Physical gelation in a triblock copolymer solution: *In situ* study of stress–strain behavior and structural development. *Macromolecules* 31:5805.

17. Kleppinger, R., N. Mishenko, H. Reynaers, and M. H. J. Koch. 1999. Long-range order in physical networks of gel-forming triblock copolymer solutions. *J. Polym. Sci. Pol. Phys.* B37:1833.

18. Wilkinson, A. N., M. L. Laugel, V. M. Clemens, V. M. Harding, and M. Marin. 1999. Phase structure in polypropylene/PA6/SEBS blends. *Polymer* 40:4971–4975.

19. Asthana, S., and J. P. Kennedy. 2002. Novel polyisobutylene stars. XXIII. Thermal, mechanical and processing characteristics of poly(phenylene ether)/polydivinylbenzene(polyisobutylene-b-polystyrene)$_{37}$ blends. *J. Appl. Polym. Sci.* 86:2866–2872.

20. Litmanovich, A. D., N. A. Platé, and Y. V. Kudryavtsev. 2002. Reactions in polymer blends: Interchain effects and theoretical problems. *Prog. Polym. Sci.* 27:915–970.

21. Laurer, J. H., J. Mulling, S. A. Khan, R. Spontak, and R. Bukovnik. 1998. Thermoplastic elastomer gels. I. Effects of composition and processing on morphology and gel behavior. *J. Polym. Sci. Pol. Phys.* B36(13):2379.

22. Laurer, J. H., J. Mulling, S. A. Khan, R. Spontak, and R. Bukovnik. 1998. Thermoplastic elastomer gels. II. Effects of composition and temperature on morphology and gel rheology. *J. Polym. Sci. Pol. Phys.* B36(14):2513–2523.

23. Dezhen, W., X. Wang, and R. Jin. 2004. Toughening of poly(2,6-dimethyl-1,4-phenylene oxide)/nylon 6 alloys with functionalized elastomers via reactive compatibilization: Morphology, mechanical properties and rheology. *Eur. Polym. J.* 40:1223–1232.

24. Wang, J., M. D. Calhoun, and S. J. Severtson. 2008. Dynamic rheological study of paraffin wax and its organoclay nanocomposites. *J. Appl. Polym. Sci.* 108:2564–2570.

25. Pracella, M., M. Haque, and V. Alvarez. 2010. Functionalization, compatibilization and properties of polyolefin composites with natural fibers. *Polymers* 2:554–574.

26. Horiuchi, S., N. Matchariyakul, K. Yase, and T. Kitano. 1997. Compatibilizing effect of maleic anhydride functionalized SEBS triblock elastomer through a reaction induced phase formation in the blends of polyamide6 and polycarbonate: 2. Mechanical properties. *Polymer* 38(1):59–78.

27. Wilkinson, A. N., M. L. Clemens, and V. M. Harding. 2004. The effect of SEBS-g-maleic anhydride reaction on the morphology and properties of polypropylene/PA6/SEBS ternary blends. *Polymer* 45:5239–5249.

28. Huang, J. J., H. Keskkula, and D. R. Paul. 2006. Elastomer particle morphology in ternary blends of maleated and non-maleated ethylene-based elastomers with polyamides: Role of elastomer phase miscibility. *Polymer* 47:639–651.

29. Chow, W. S., Y. Y. Leu, and Z. A. Mohd Ishak. 2012. Effects of SEBS-g-MAH on the properties of injection moulded poly(lactic acid)/nano-calcium carbonate composites. *Express Polym. Lett.* 6(6):503–510.

30. Maruizumi, H., K. Kosaka, S. Suzuki, and D. Fukuma. 1988. Development of HTPB binder for solid propellants. AIAA Paper No. 88-3352.

31. Haska, S., E. Bayramli, F. Pekel, and S. Ozkar. 1996. Mechanical properties of HTPB-IPDI-based propellants. *J. Appl. Polym. Sci.* 64:2347–2354.

32. Vilar, W., and L. Akcelrud. 1995. Effect of HTPB structure on prepolymer characteristics and on mechanical properties of polybutadiene-based polyurethanes. *Polym. Bull.* 35:635–639.

33. Asadchii, O. G., B. Z. Votlokhin, N. F. Bogdanov, and V. P. Gladyshev. 1979. Determination of tensile strength of paraffin waxes. *Khimiya i Tekhnologiya Topliv i Masel* 10:51–53.

34. Wang, J., S. J. Severtson, and A. Stein. 2006. Significant and concurrent enhancement of stiffness, strength, and toughness for paraffin wax through organoclay addition. *Adv. Mater.* 18:1585–1588.

35. Pu, G., J. Wang, and S. J. Severtson. 2007. Properties of paraffin wax/montmorillonite nanocomposite coatings. *NSTI Nanotechnology Conference and Trade Show Technical Proceedings*. Santa Clara, CA. 2:112–115.

36. DeSain, J. D., B. B. Brady, K. M. Metzler, T. J. Curtiss, and T. V. Albright. 2009. Tensile tests of paraffin wax for hybrid rocket fuel grains. AIAA Paper No. 2009-5115.